

Development of Doppler radar wind data assimilation for the HIRLAM 3D-Var

M. Lindskog^{1,*}, H. Järvinen², D. B. Michelson¹

¹*Swedish Meteorological and Hydrological Institute, S-60176 Norrköping, Sweden*

²*Finnish Meteorological Institute, Helsinki, Finland*

February 4, 2002

* *Corresponding author, email: Magnus.Lindskog@smhi.se*

Abstract

A three-dimensional variational data assimilation (3D-Var) scheme has been developed for the High Resolution Limited Area Model (HIRLAM). The HIRLAM 3D-Var minimizes a cost function measuring the distance of the analysis to the background field and to the observations. Each source of information is weighted according to its estimated error covariance. Radar wind observations can be input for HIRLAM 3D-Var either as radial wind super-observations or as vertical profiles of horizontal wind obtained with the Velocity Azimuth Display (VAD) technique. Background error standard deviation (σ_b) of wind and radial wind have been estimated by applying a randomization method, in which the background state is perturbed with Gaussian errors. The derived values of σ_b are used in the quality control of observations, and also in the assignment of radar wind observation error standard deviations (σ_o). Parallel data assimilation and forecast experiments confirm reasonably well-tuned error statistics and indicate a slightly positive impact of radar wind data on the verification scores, regardless of whether the radar wind information is input as radial wind super-observations or as VAD wind profiles.

1 Introduction

Data assimilation in numerical weather prediction optimally blends observations with an atmospheric model in order to obtain the spatial distribution of atmospheric variables and to produce the best possible model initial state. The number of observations is in general small compared to the number of degrees of freedom in the initial state of the forecast model. To overcome this problem one introduces so-called a *priori* information. The *a priori* information is in the form of a short-range forecast and statistical knowledge about the errors of this forecast, in addition to statistical knowledge about the error of the observations. One may also utilize additional pieces of a *priori* information, regarding, for example, balances between different forecast model variables.

Due to improved assimilation techniques, increased model resolutions and more developed infrastructure for data communication, the interest in assimilation of wind data from Doppler weather radars has recently increased. Research and co-operation within this area is also stimulated through the European COST 717 action concerning “Use of Radar Observations in Hydrological and NWP models” (Rossa, 2000). The radial wind data can in principle be assimilated directly into the atmospheric models, but in practice different processing¹ methods are applied before the data are passed to the atmospheric models. The Velocity Azimuth Display (VAD) technique can be used as one such processing method; it provides vertical profiles of horizontal winds from the raw radial wind data (Lhermitte and Atlas, 1961; Browning and Wexler, 1968; Andersson, 1992). Another form of processing is to generate radial wind super-observations through methods based on spatial averaging. The super-observations will be smoother than the raw data and representative of a spatial scale depending on the averaging procedure. With super-observations, the spatial structures within the domain of each radar will be accounted for. The handling of radar wind observations requires a quality control system to remove data contaminated by for example clutter as well as velocity ambiguities.

Radar wind data in the form of radial wind super-observations have been assimilated in research mode with the 3D-Var scheme of the National Centers for Environmental Prediction (NCEP) ETA forecasting system (Parrish and Purser, 1998), the 4-dimensional Variational Doppler Radar Analysis System (VDRAS) developed by Sun and Crook (1997) at the National Center for Atmospheric Research (NCAR), and recently within an earlier version of the HIRLAM 3D-Var (Lindskog et al., 2000). Radar data in the form of VAD wind profiles have been assimilated in research mode by different groups but have also been assimilated operationally within the Optimal Interpolation (OI) and 3D-Var schemes of the NCEP ETA forecasting system (Parrish, personal communication) and VAD wind profiles are presently being assimilated into an operational meso-scale assimilation and forecasting system at The Met. Office (Macpherson, personal communication) through the nudging method.

An operationally suitable 3D-Var scheme for the HIRLAM forecasting system has been developed (Gustafsson et al., 2001; Lindskog et al., 2001) and it is based on a mini-

¹In radar engineering terminology, “pre-processing” is synonymous with signal processing. What meteorological modelers refer to as “pre-processing” is referred to as “post-processing” in radar meteorology. We propose a simplification of the respective terminologies such that the preparation of radar data prior to assimilation in models be referred to as “processing”.

mization of a cost function that consists of one term measuring the distance between the resulting analysis and a background field, which is a short-range forecast, and another term measuring the distance between the analysis and the observations. The present version of the HIRLAM 3D-Var has been prepared for assimilation of Doppler radar wind data either as radial wind super-observations or as VAD wind profiles. The observation handling system has been extended and investigations, as well as tuning, of radar wind error statistics have been performed. The error studies made use of a randomization method, which involves perturbing the background state with Gaussian errors and propagation of these errors to observation space. To get an indication of the potential benefit of radar wind data and to estimate the effects of the choice of processing method (radial wind super-observation or VAD wind profile), a ten-day parallel data assimilation and forecast experiment has been performed.

In Section 2 the HIRLAM 3D-Var is briefly described, followed by an overview of the observation processing system, with emphasis on radar winds, in Section 3. Estimation of radar wind error statistics by applying a randomization method is the subject of Section 4. Section 5 is concerned with parallel data assimilation and forecast experiments, utilizing radar wind data from the Swedish Doppler radar network. A discussion and some concluding remarks are presented in Section 6.

2 The HIRLAM 3D-Var

The HIRLAM 3D-Var has an incremental formulation and the assimilation consists in minimizing the following cost function

$$J = J_b + J_o = \frac{1}{2}\delta\mathbf{x}^T\mathbf{B}^{-1}\delta\mathbf{x} + \frac{1}{2}(\mathbf{H}\mathbf{x}^b + \mathbf{H}\delta\mathbf{x} - \mathbf{y})^T\mathbf{R}^{-1}(\mathbf{H}\mathbf{x}^b + \mathbf{H}\delta\mathbf{x} - \mathbf{y}). \quad (1)$$

Here J_b measures the distance to a background model state \mathbf{x}^b , which is a short range forecast, and J_o measures the distance to the vector \mathbf{y} of the observations. The non-linear observation operator H and the tangent-linear observation operator \mathbf{H} transform the background state and assimilation increments, respectively, into the observed quantities. \mathbf{B} is the matrix containing the covariances of the background field errors, while \mathbf{R} is a matrix containing the covariances of the errors in the observations. For HIRLAM the model state increment vector $\delta\mathbf{x}$, includes the horizontal wind components, temperature, specific humidity and the logarithm of surface pressure.

Background error statistics are derived from a sample of differences between forecasts valid at the same time (Parrish and Derber, 1992) and with a non-separable approach (the vertical variability of horizontal correlations and the dependence of vertical correlations on horizontal scale are represented).

The observation operator H and the tangent-linear observation operator \mathbf{H} are subdivided into a sequence of sub-operators. For the non-linear observation operator we may formally write

$$H = H_{spec}I_vP_{calc}I_hF^{-1}, \quad (2)$$

where F^{-1} is an inverse Fourier transform, I_h denotes horizontal interpolation of model data from grid points to the horizontal positions of the observations, P_{calc} calculation

of pressures and geopotentials at model full and half levels, I_v vertical interpolation to the levels of the observed data values and H_{spec} any other specific operators for each type of observation. For the non-linear observation operator the inverse Fourier transform is carried out only when the HIRLAM 3D-Var is applied together with a spectral forecast model. An expression corresponding to (2) exists for the tangent-linear observation operator. At present observation operators have been developed for various conventional data, as well as for data from TOVS (TIROS Operational Vertical Sounder) and ATOVS (Advanced TOVS) radiances, GPS (Global Positioning System) atmospheric delays, GPS occultations, scatterometers, Doppler radar VAD wind profiles and radial winds. The observation errors are assumed to be uncorrelated for all observation types (except for a possibility to account for correlations between radiance errors in different ATOVS channels). With this assumption, the covariance matrix \mathbf{R} for the observation errors becomes a diagonal matrix and only the observation error standard deviations (σ_o) need to be specified (Lindskog et al., 2001).

A standard minimization software package (Gilbert and Lemaréchal, 1989), based on an iterative technique, is used to find the minimum of J with respect to the analysis increment $\delta\mathbf{x}$. For each iteration, the gradient of the cost function with respect to the model state increment vector $\delta\mathbf{x}$ is calculated by

$$\nabla_{\delta\mathbf{x}}J = \mathbf{B}^{-1}\delta\mathbf{x} + \mathbf{H}^T\mathbf{R}^{-1}(H\mathbf{x}^b + \mathbf{H}\delta\mathbf{x} - \mathbf{y}). \quad (3)$$

In order to obtain a fast convergence of the minimization a pre-conditioning for the HIRLAM 3D-Var is introduced in the form of a series of transforms, \mathbf{U} , that is applied to the analysis increments. It includes 2-dimensional horizontal Fourier transforms, subtraction of the geostrophic wind increments and projection on eigen-vectors of vertical background error correlation matrices. The transformations result in an assimilation control variable, χ , for which the background error covariance matrix can be assumed to be an identity matrix, and the expression for the cost function becomes

$$J = J_b + J_o = \frac{1}{2}\chi^T\chi + \frac{1}{2}(H\mathbf{x}^b + \mathbf{H}\mathbf{U}^{-1}\chi - \mathbf{y})^T\mathbf{R}^{-1}(H\mathbf{x}^b + \mathbf{H}\mathbf{U}^{-1}\chi - \mathbf{y}), \quad (4)$$

where

$$\chi = \mathbf{U}\delta\mathbf{x} \quad (5)$$

is the formal expression for the transformations (\mathbf{U}) that relates $\delta\mathbf{x}$ to χ .

3 Processing of Doppler radar wind data

3.1 Radars

A Doppler weather radar is an active remote sensing instrument which transmits electromagnetic wave pulses and receives reflected echoes in order to investigate the properties of the atmosphere. The amplitude of the returning wave pulses is used to estimate the reflectivity which can be related to precipitation intensity. The phase shift between the transmitted and received pulses, i.e. the Doppler shift, is used to estimate the radial wind. The radar measurements are unfortunately limited in the sense that there is

a trade-off between the maximum unambiguous velocity, V_a , and the maximum unambiguous range, R_a . The unambiguous range R_a is related to the rate at which the radar transmits, i.e. the Pulse Repetition Frequency (PRF), and also to the propagation speed of the transmitted electromagnetic wave (c) through

$$R_a = \frac{c}{2 PRF}. \quad (6)$$

The ambiguity velocity is dependent on the PRF , and on the wavelength (λ) of the signal

$$\pm V_a = \pm \frac{\lambda PRF}{4}. \quad (7)$$

Thus R_a and V_a are related through

$$R_a V_a = \frac{c \lambda}{8}. \quad (8)$$

Obviously, for a fixed λ (in accordance with what is technically and practically attainable) in (8) an increase of R_a can only be achieved by decreasing V_a .

The Swedish radar network consists of 12 Ericsson C-band systems. All Swedish radars have a λ of approximately 5.3 cm (5.65 GHz) and are operated with dual PRF of 900 and 1200 Hz, respectively. According to (6) to (8) these values should result in R_a and V_a of 167 km and ± 11.9 m/s, respectively, for 900 Hz and 125 km and ± 15.9 m/s, respectively, for 1200 Hz. However, a staggering of the two different PRF s is used to effectively increase the composite velocity unambiguity value (Doviak and Zrinc, 1993). The resulting range and velocity composite unambiguity values (R_{ac} and V_{ac}) are 120 km and ± 48 m/s, respectively. This established procedure of staggering PRF s is, however, not widely utilized in European weather radar networks.

The raw Swedish radar data have a resolution in the azimuth dimension of 0.9° (420 per scan) and in range of 1 km (120 per azimuth gate). For geometrical reasons, this will of course result in a higher density of raw data closer to the radar than at more distant ranges. Another related issue is the broadening of the radar beam with increased range from the radar. The half-power beamwidth of a pulse is the distance from the central axis of the pulse to the point where the intensity has dropped by -3 dB from its value at the central axis. Swedish radars collect data in a sequence of scans with increasing elevation angle, repeated every 15 minutes.

3.2 Data processing and flow

The observation handling system of the HIRLAM 3D-Var is designed to handle a variety of different data types, computer architectures and to manage data volumes associated with a limited area assimilation system. An overview of the system, with main emphasis on handling of radar wind data, is given in Fig. 1. Raw radar wind data are passed either through the processing algorithm for generation of radial wind super-observations in ASCII format (initially considered as the HIRLAM 3D-Var main strategy) or through the algorithm for generation of VAD wind profiles in ASCII format (here denoted as an alternative strategy).

Either type of ASCII observation file can be passed to the observation processing routine MAKECMA together with other types of observations that are normally in BUFR (Binary Universal Form for the Representation of meteorological data) format. The MAKECMA module processes the observations and an observation data file in the Central Memory Array (CMA) format, which is designed to be suitable for use in variational data assimilation (Saarinen et al., 1997). The processing includes quality control and thinning of the radar radial wind super-observations, crude checks of other types of data and, if necessary, observed variables are transformed into those used directly by the variational assimilation. The σ_o values are assigned during this step. The main tasks of the screening are quality control using various algorithms, including a comparison with the background field, data rejections and data thinning to select only those observed values that will actually be used by the variational data assimilation. The remaining data are passed to the variational data assimilation calculations.

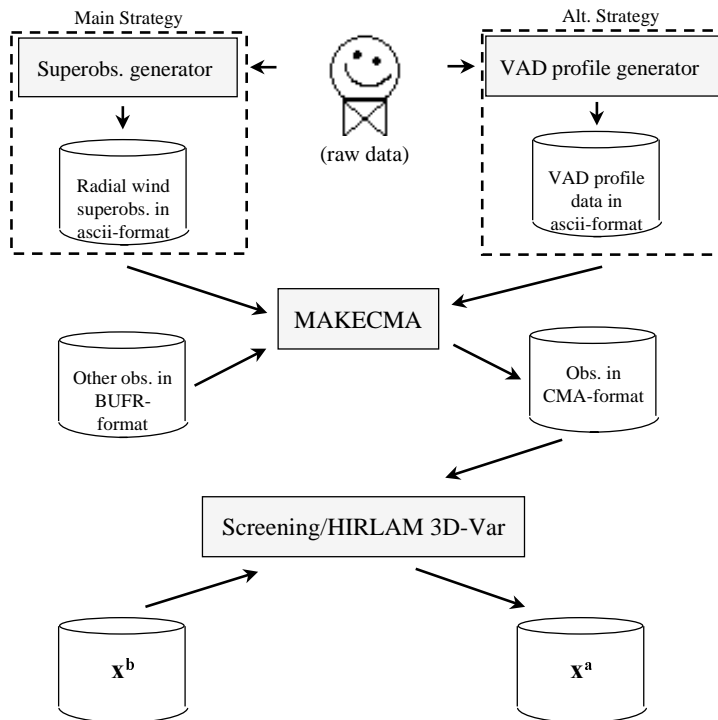


Figure 1: Overview of the HIRLAM 3D-Var observation processing system, including radar processing algorithms. Modules are represented by boxes and files by cylinders.

The processing software used to generate radar super-observations has been developed as an extension module to the Radar Analysis and Visualization Environment (Michelson, 1999). Radial wind super-observations are generated through horizontal averaging in polar space of the raw polar volume of data. The polar-to-polar transformation is based on a strategy for improved polar-to-cartesian transformation (Henja and Michelson, 1999). To minimize horizontal correlations of the super-observations, each piece of raw data is allowed to influence one super-observation only. To avoid averaging of radial winds with significantly different directions the averaging search radius is a function of distance from the radar. The radius is larger at large distances from the radar, as compared to shorter distances from the radar. The horizontal averaging when generating the super-observations is illustrated in Fig. 2. To minimize vertical correlations of the super-observations two scans are constrained not to overlap. Such

non-overlapping scans are iteratively determined such that, starting with the lowest scan, the closest non-overlapping scan is identified and super-observations are generated through horizontal averaging; this scan then becomes the starting point and the closest non-overlapping scan to it is found. This continues until the highest allowed elevation angle is reached. A number of supporting variables are derived and written to a file, radial wind variances being among them.

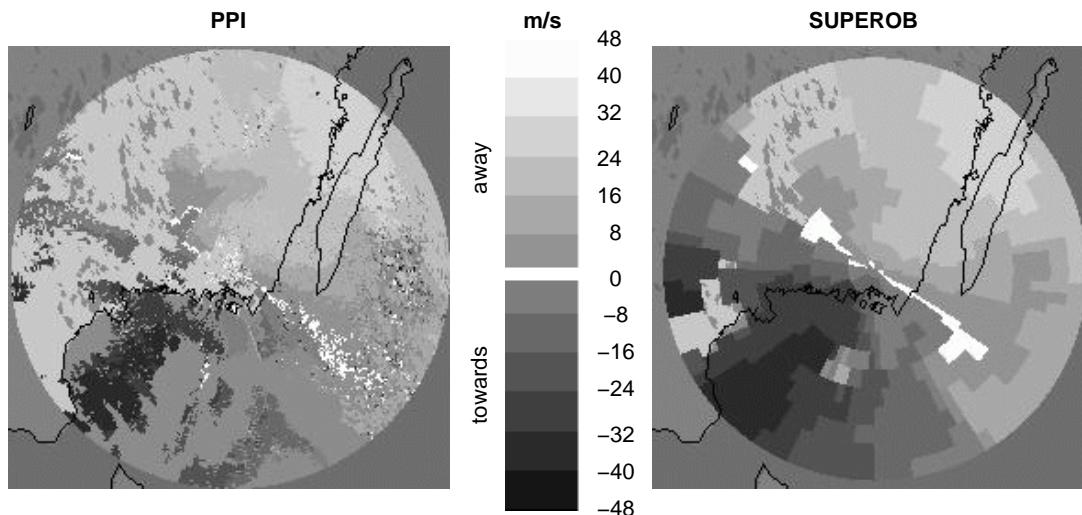


Figure 2: Radial wind raw data (left) and super-observations generated through horizontal averaging (right).

A slightly modified version of that developed by Andersson (1992) is used to process a given polar volume data to one VAD horizontal wind profile. This implementation of the VAD algorithm is used routinely at the BALTEX (BALTic sea EXperiment) Radar Data Centre (Michelson et al., 2000) and the maximum horizontal radius of the VAD circle is 25 km. The VAD circle and schematics is presented in Fig. 3.

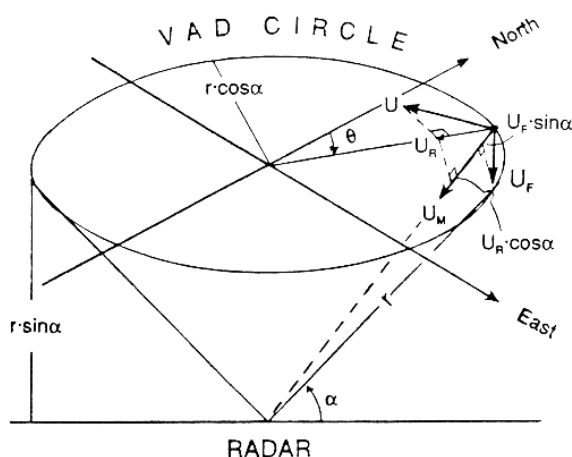


Figure 3: VAD circle with associated variables. From Andersson (1992).

3.3 The radar wind observation operators

The radar wind observation operator produces the model counterpart of the observed quantity that is presented to the variational assimilation. In the case of a horizontal wind observation from VAD profiles the observation operator consists of a simple interpolation of the model wind field to the location of the observation (I_v , P_{calc} , I_h and F^{-1} in (2)). If the observed quantity is a radar radial wind super-observation, which is not a model variable, the observation operator includes also a specific observation operator (H_{spec} in (2)). The specific observation operator for the radial wind super-observations involves first a projection of the model horizontal wind at the point of the measurement in the direction towards the radar

$$v_h = u \sin \theta + v \cos \theta. \quad (9)$$

Here θ is the azimuth angle of the radar beam, relative to the local y-direction of the model. v_h is then projected on the slanted direction of the radar beam by

$$v_r = v_h \cos(\phi + \alpha). \quad (10)$$

Here ϕ is the elevation angle of the radar beam, and α is calculated from the following formula

$$\alpha = \arctan \left(\frac{d \cos \phi}{d \sin \phi + r + h} \right), \quad (11)$$

where d is for the range of the measurement from the radar, r is for the radius of the Earth and h is for the height of the radar above mean sea level, respectively. The α -term in the projection in (11) accounts in an approximate way for the Earth's curvature.

Two major assumptions are built into this formulation of the observation operator. First, it is assumed that the measured radial wind is point-wise representative. The formulation of the observation operator must be regarded as a first approximation, since it is well known that the radar beam broadens with increasing range from the radar. Second, it is assumed that the projection of the vertical velocity on the radar beam is negligible. This assumption implies that the observation operator is only applicable for assimilation of low elevation angle radar data.

3.4 Quality control

The MAKECMA observation processing module involves an extended quality control of radial wind super-observations and also a thinning of these data. To ensure that a super-observation is representative of a volume somewhat larger than a single original polar bin, it is rejected if it consists of data from less than five original polar bins or if it has a variance larger than $10 \text{ m}^2/\text{s}^2$. Since we want to minimize the influence of the vertical radial wind component, an upper threshold of 10° is set on accepted elevation angles. Due to the fact that the radar beam broadens vertically (as much as it does horizontally) with increasing range from the radar, while the super-observation is presently treated as a point-source in the HIRLAM 3D-Var, the maximum range

is set to 100 km. This vertical broadening is shown in Fig. 4, which illustrates the vertical extent of the half-power (-3 dB) beamwidth.

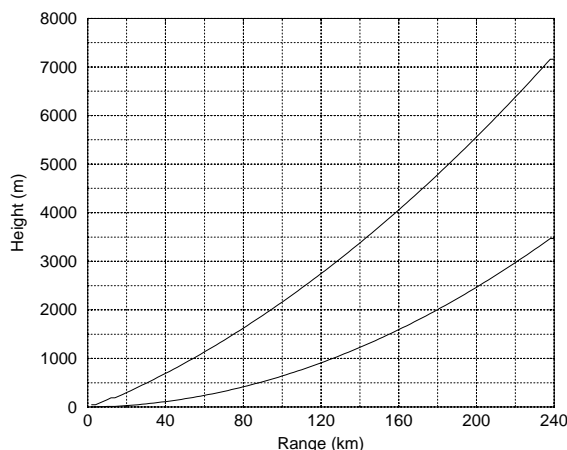


Figure 4: Vertical propagation of a one degree radar beam transmitted with an elevation angle of 0.5° , assuming a half-power (-3 dB) beamwidth, as a function of range from the radar.

As a sanity check related to the unambiguous velocity interval of the Swedish Doppler radars, no super-observations with wind speeds larger than 50 m/s are accepted. Data that pass the previous checks are thinned. Super-observations originating from the same radar and being at the same ranges from the radar are considered redundant if their azimuth angles deviate by less than 12° . If two super-observations are considered redundant, the one with the smallest variance is accepted. The functionality of the thinning is demonstrated in Fig. 5, for a particular case.

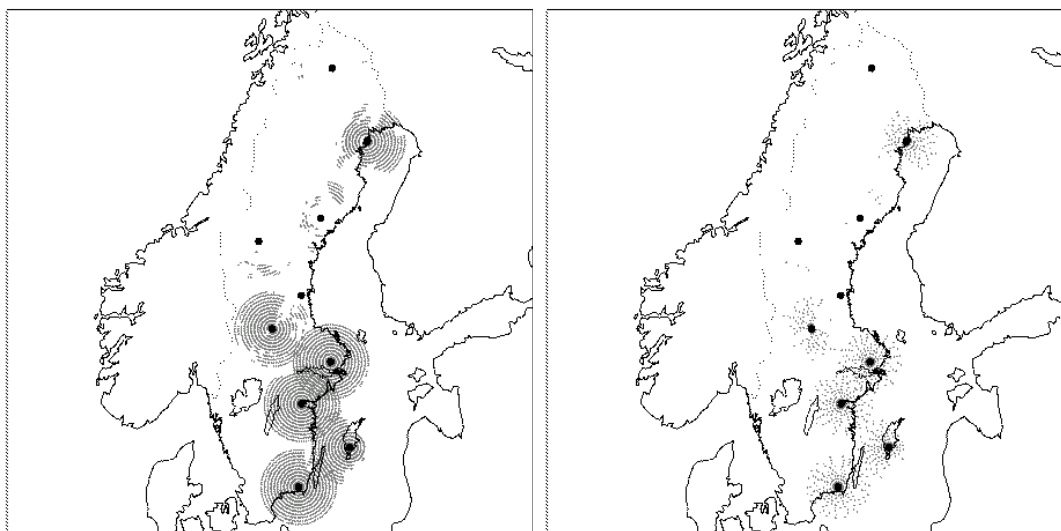


Figure 5: Illustration of thinning of radar radial wind super-observations for the particular case of 6 December 1999 12 UTC. Big black dots represent the radar sites and small grey dots the super-observations before (left panel) and after (right panel) thinning.

All radar radial wind super-observations and VAD wind observations that pass the

former quality control steps are subject to a background quality control, in which the *a priori* information in the background state is utilized. Each individual radial wind super-observation, y_i , is checked against the background value, $[H(\mathbf{x}^b)]_i$. An observation is passed to the minimization if the inequality

$$L_1 \leq \frac{|[H(\mathbf{x}^b)]_i - y_i| ([H(\mathbf{x}^b)]_i - y_i)}{\sigma_{b,i}^2 + \sigma_{o,i}^2} \leq L_2 \quad (12)$$

is fulfilled, where L_1 and L_2 are the upper and lower rejection limits and $\sigma_{b,i}$ and $\sigma_{o,i}$ denote the background error standard deviation and the observation error standard deviation, respectively, of observation i . In the case of radial wind super-observations the values -6 and 6 are used for L_1 and L_2 , respectively. In the case of VAD wind profiles, both components are checked jointly and an observation is passed to the minimization if the inequality

$$L_1 \leq \frac{1}{2} \left(\left[\frac{|[H(\mathbf{x}^b)]_i - y_i| ([H(\mathbf{x}^b)]_i - y_i)}{\sigma_{b,i}^2 + \sigma_{o,i}^2} \right]_u + \left[\frac{|[H(\mathbf{x}^b)]_i - y_i| ([H(\mathbf{x}^b)]_i - y_i)}{\sigma_{b,i}^2 + \sigma_{o,i}^2} \right]_v \right) \leq L_2, \quad (13)$$

is fulfilled, where the L_1 and L_2 values are -8 and 8, respectively. The values of the L_1 and L_2 parameters are rather arbitrarily chosen, both for super-observations and VAD winds. For the values of $\sigma_{b,i}$ and $\sigma_{o,i}$ we refer to Section 4.

For wind observations above 700 hPa and for wind speeds greater than 15 m/s, a wind direction check is applied. If more than four consecutive VAD levels are flagged as suspicious, all of these data are rejected.

Finally, the minimization itself contains a so-called variational quality control (Lorenc and Hammon, 1988; Ingleby and Lorenc, 1993; Andersson and Järvinen, 1999), that accounts for non-Gaussian observation errors in radar wind data, as well as in other data. The variational quality control for radar wind data involves two parameters representing the range of possible values and the probability of gross errors. For radar wind data, we have initially used the parameter values derived for PILOT balloon reports. These values are based on investigation of statistics files from the INM (Spanish Meteorological Institute) operational OI analysis (Gustafsson et al., 1999).

4 Estimation of radar wind error statistics

The σ_b values of the variables contained in the model state increment vector (ageostrophic wind components, temperature, specific humidity and logarithm of surface pressure) are specified in the HIRLAM 3D-Var. The σ_b for the full wind field and other quantities that are not contained in the model state increment vector, such as Doppler radar radial wind, need to be experimentally determined. Furthermore, the radar wind σ_o values need to be specified in order to assure realistic weights for the radar wind observations in the assimilation with respect to other sources of information. Apart from the importance of the σ_b/σ_o values for assigning weights in the assimilation

procedure, they are required in the background quality control, as described in Section 3.4.

The background errors in VAD wind observation space (which are very similar to the errors of the full wind in grid point space) and in radial wind observation space may be calculated by supplying the control vector χ , with Gaussian errors with zero mean and standard deviation equal to one. The control vector is then transformed into the observation space by applying the inverse of the series of transforms described in Section 2, followed by a projection by the observation operator. A large number of such randomizations give an estimate of the background error standard deviations in observation space ($\hat{\sigma}_b$) by

$$\hat{\sigma}_b = \sqrt{\frac{1}{N} \sum_{i=1}^N (H\mathbf{U}^{-1}\chi_i)^2} \quad (14)$$

where \mathbf{U}^{-1} is the inverse of the series of transforms, H is the observation operator, N is the sample size and χ_i is the control vector (containing Gaussian errors) for the individual sample member i .

The randomization method yields $\hat{\sigma}_b$ for radar wind data. A sample of 500 random χ_i -vectors is used and at each grid-point H corresponding with VAD wind profiles and with radar radial winds, respectively, are applied in (14). The final value of $\hat{\sigma}_b$ is a horizontal average over all grid points of a model level. This averaging procedure can be justified by noting that the horizontal variations of $\hat{\sigma}_b$ are small compared with the vertical variations and thus a $\hat{\sigma}_b$ profile describes most features. The resulting vertical profile of $\hat{\sigma}_b$ can be regarded as a good approximation of σ_b in VAD wind observation space.

The vertical profile of $\hat{\sigma}_b$ for total wind averaged in grid point space is shown in Fig. 6 (left panel) together with the σ_o specified for VAD and for radar radial wind observations. Note that the σ_o values have been assumed to be constant. The specified σ_o for the VAD wind observations is of the same order of magnitude as $\hat{\sigma}_b$. The specified σ_o for the radial wind super-observations is 50% larger than for VAD observations. Thus the impact of a single radial wind super-observation is less than the impact of a single VAD wind observation. This choice may be theoretically justified by the fact that the VAD profiles are more strongly filtered than the radial wind super-observations. The representativity error at 22 km model horizontal resolution should therefore be smaller for VAD wind than for radial wind observations. An additional justification for the larger specified σ_o value of radar radial wind super-observations is an attempt to account for the large number of super-observations in each assimilation cycle and to avoid a domination of radial wind super-observations at the expense of other sources of information. Due to the procedure for data selection in the processing algorithms and for simplicity reasons, the observation errors of radar wind data are assumed to be spatially uncorrelated, both for radial wind super-observations and VAD wind profiles.

In the radar radial wind observation space, the effect of the specific observation operator on the σ_b value is minute for small elevation angles and for short ranges. There is a weak dependency of $\hat{\sigma}_b$ on range. This is due to the fact that the specific observation operator accounts for the curvature of the earth. The dependency of $\hat{\sigma}_b$ on radar elevation angle is due to the projection of the local horizontal wind on the slanted path of the radar beam, as described by (10). $\hat{\sigma}_b$ in radar radial wind observation space

is proportional to the cosine of the radar antenna elevation angle. Keeping in mind that only radar radial wind super-observations with elevation angles smaller than 10° are passed through the observation screening to the assimilation, the $\hat{\sigma}_b$ variations are fairly unimportant.

Figure 6 (right panel) illustrates the dependency of $\hat{\sigma}_b$ in radial wind observation space on the radar antenna elevation angle and on the range. The dependency is weak on small elevation angles. The $\hat{\sigma}_b$ decreases with increasing elevation angle. It would thus seem that the larger the radar elevation angle, the more accurate the model background becomes. The interpretation of the result is, however, that with large elevation angles, the model counterpart, i.e. $H\mathbf{x}^b$, depends less on model horizontal wind and errors in it.

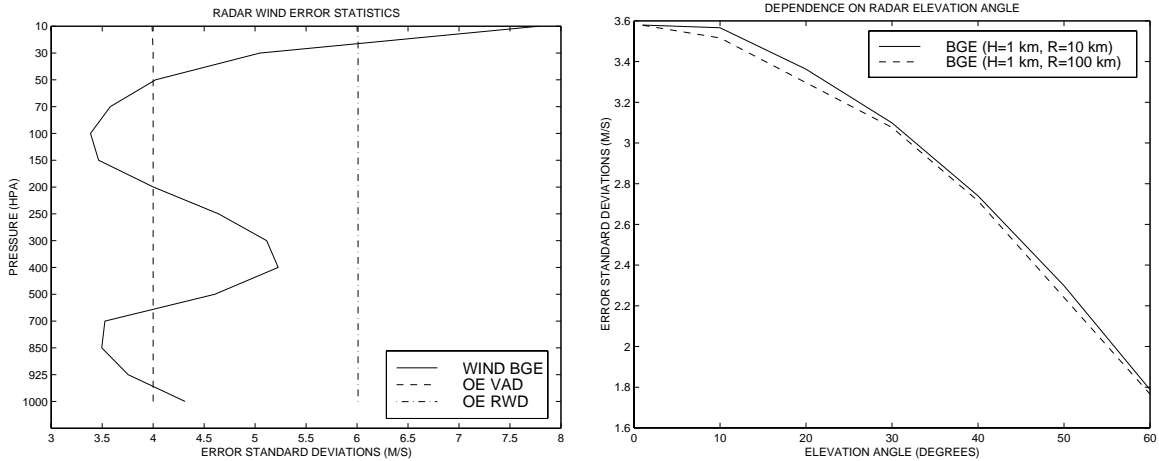


Figure 6: Vertical profile of horizontally averaged wind σ_b and the specified radar VAD and radial wind σ_o 's (left). Dependency of $\hat{\sigma}_b$ in radial wind space of the elevation angle and of the distance from the radar site (right). Unit [m/s].

Perhaps a more objective way to derive σ_o for radar wind data would be to compare the innovation vector ($\mathbf{y} - H\mathbf{x}^b$) of radar wind data with the σ_b values and with co-located radiosonde or aircraft wind observations, with better known σ_o values.

A demanding problem is to account for the possible spatial correlation of the raw radial wind observation errors. The first task would be to accurately describe the observation error correlations. The second task would be a technical one. The HIRLAM 3D-Var, like most assimilation systems, is not designed to properly account for these correlations, although it is theoretically possible. The difficulties of correlated observation errors have generally been circumvented in data assimilation by applying data selection and thinning algorithms, or observation processing algorithms that are assumed to remove the observation error correlations. There is ongoing research in this area (Lin et al., 2000).

5 Assimilation experiments

5.1 Experimental design

A ten-day assimilation and forecast experiment, extending from 1 to 10 December, 1999, has been performed over an area covering Northern Europe and the Northern Atlantic. Synoptically the period is characterized by deep cyclones passing over the Baltic Sea area. The three parallel data assimilation experiments are characterized as follows:

- 1) Only conventional observations are used.
- 2) Conventional observations and VAD wind profiles based on data from the Swedish radar network are used.
- 3) Conventional observations and radial wind super-observations based on data from the Swedish radar network are used.

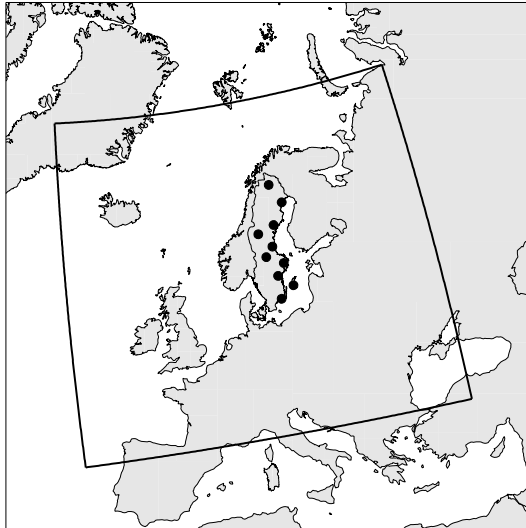


Figure 7: Model integration area and the Swedish radar sites utilized in the study.

The conventional observations are retrieved from the ECMWF (European Centre for Medium Range Weather Forecasts) archive and the radar data from the BALTEX Radar Data Centre (Michelson et al., 2000). The model integration area and the location of the Swedish radars used in the study are illustrated in Fig. 7. After each analysis, a non-linear normal mode initialization is applied (Machenhauer, 1977), followed by a +30 h forecast. For the lateral boundary conditions, three-hourly ECMWF 4D-Var analyses are used. The assimilation experiments are carried out with the spectral HIRLAM forecast model. The model integration area consists of 162×142 horizontal grid points at 0.2° resolution and 31 vertical levels. The physics package included a first order local vertical diffusion scheme (Louis, 1979), a cloud and condensation scheme based on explicit forecasts of cloud water (Sundqvist et al., 1989) and a radiation scheme based on Savijärvi (1989). Eulerian time integration and a fourth order implicit horizontal diffusion scheme are used in all model integrations.

5.2 Case study

In order to illustrate the impact of the radar wind data on a single analysis, the analysis of the first assimilation cycle is studied in detail. This assimilation cycle of all parallel data assimilation experiments utilizes the same background field, which is a +6 h forecast launched from an ECMWF analysis. Fig. 8 shows the difference between the analysis using conventional observations only and the analyses using radar winds in addition to the conventional observations.

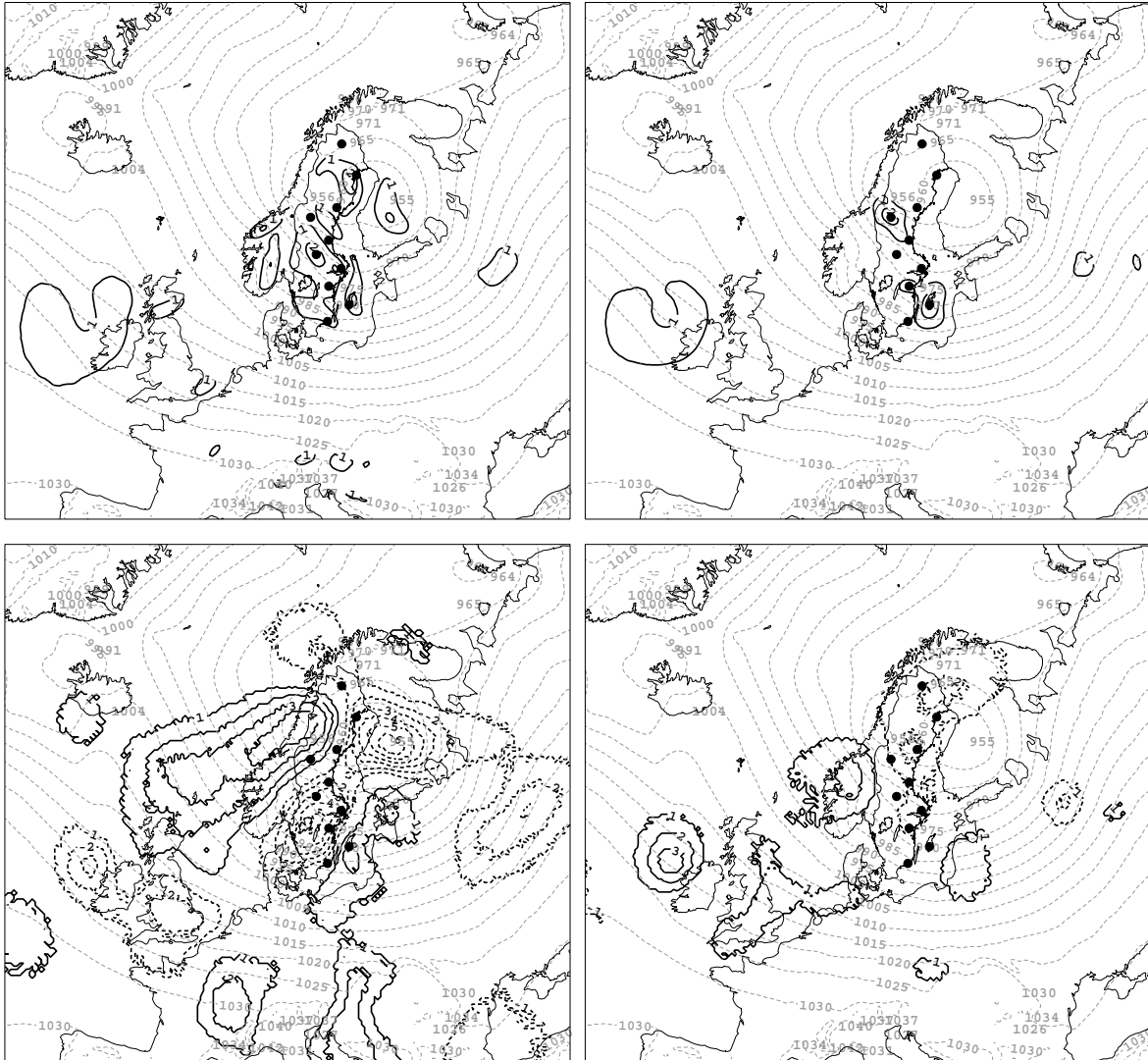


Figure 8: The difference between the analysis utilizing conventional data only and the analyses utilizing in addition radial wind super-observations (left column) or radar VAD profiles (right column). Full lines in the upper row show the model level 31 (lowest model level) wind speed differences in m/s. Full lines in the lower row show the model level 29 temperature field differences in tenths of K. The Mean Sea Level Pressure (MSLP) of the analysis utilizing conventional data only is shown with gray dotted line in all panels [unit: hPa]. The radar sites are denoted by black dots.

The differences are displayed for low level wind and temperature. It can be seen that the use of radar winds alters the wind speeds from those of the control run by 1-2

m/s. The major differences occur near the radar sites in Sweden. The magnitude of the analysis differences as well as the area influenced by the additional observations is larger in the case of radar radial winds as compared with the case of VAD wind profiles. In the case of VAD wind profiles the wind increments are mostly centered around a few radar sites. In both cases, however, the radar wind observations change the analysis as far away as the British Isles. The changes in wind analysis are due to the radar wind data and the effect is spread to mass and temperature analyses through the multivariate geostrophic coupling of the background error covariances. There is also a very non-linear effect on the analysis which is due to the changes in observation quality control decisions. These changes may affect the analysis over quite large distances from the actual new observational information.

5.3 Observation fit statistics

Figure 9 displays innovation ($\mathbf{y} - H\mathbf{x}^b$) and residual ($\mathbf{y} - H\mathbf{x}^a$) statistics for all radar wind observations assimilated over the ten-day period. It can be seen that the model is fairly unbiased with respect both the VAD profiles and the radial wind super-observations. The Root Mean Square (RMS) for the residuals is smaller than for the innovations.

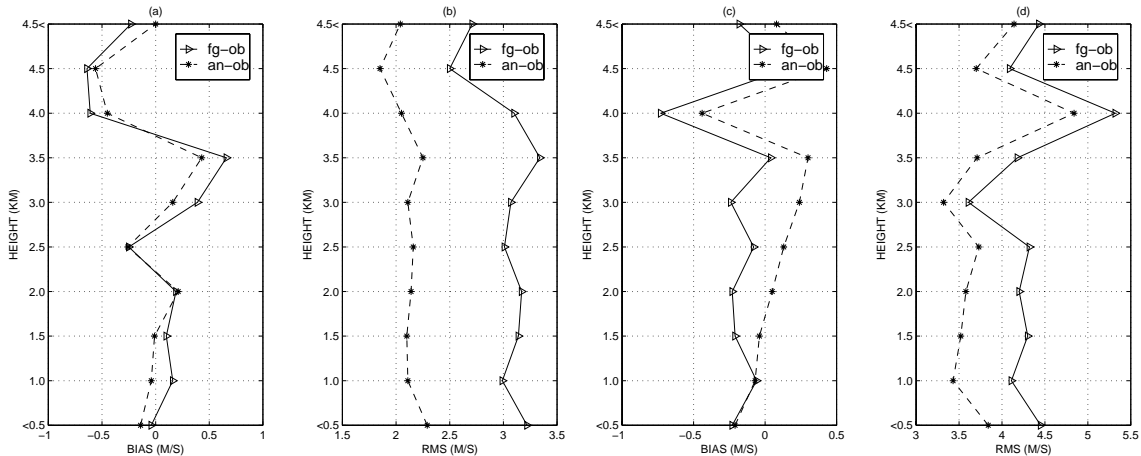


Figure 9: Innovation and residual statistics for VAD wind and radial wind super-observations used in the assimilation during 1- 10 December 1999. Bias (a) and RMS (b) of innovation (full) and residual (dashed) for radar VAD wind observations. Bias (c) and RMS (d) of innovation (full) and residual (dashed) for radar radial winds. Unit [m/s].

It is evident, in accordance with our specified error statistics, that the difference between the RMS of residuals and the RMS of innovations is larger for VAD wind observations than for wind super-observations: the analysis “draws” more closely to the VAD wind observations than to the radar radial wind observations. The RMS of residuals confirms our estimate that the σ_o of the VAD wind components are smaller than the σ_o for the radial wind super-observations. It seems however, that the assumed σ_o values of 4 m/s and 6 m/s for the VAD wind data and the radial wind super-observations, respectively, are over-estimations.

5.4 Verification against observations

In order to evaluate the impact of radar wind data in the form of VAD wind profiles and radial wind super-observations on the 3D-Var analyses and subsequent forecasts, the analyses and forecasts of the three parallel runs are verified against observations in the list of radiosonde and SYNOP stations established by the European Working Group on Limited Area Models (EWGLAM). The verification is done for 850, 700 and 500 hPa winds and temperatures, since these parameters are expected to be influenced most by the radar winds. The model data used in the statistics are the analyses and the +6, +12, +18, +24 and +30 h forecasts.

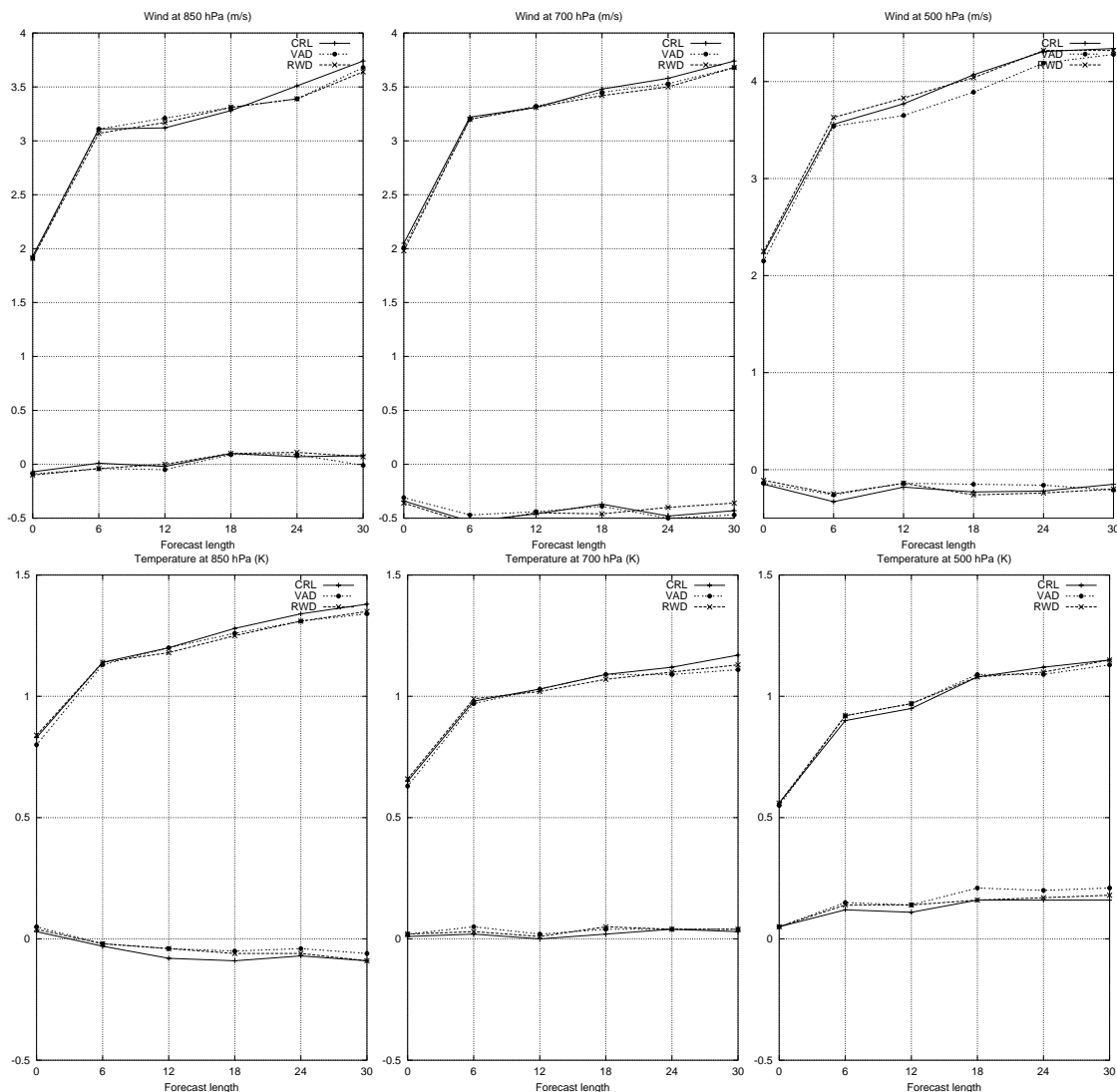


Figure 10: Average bias and RMS scores for the ten-day assimilation period (1 - 10 December 1999), as functions of forecast length (h). Wind speed scores (m/s) at 850 hPa (upper left), 700 hPa (upper middle) and 500 hPa (upper right) as well as temperature scores (K) at 850 hPa (lower left), 700 hPa (lower middle) and 500 hPa (lower right). The scores are for the run utilizing conventional observations only (full line), for the run utilizing conventional observations and VAD winds (dot-dashed), and for the run utilizing conventional observations and radar radial wind super-observations (dashed with crosses).

Figure 10 illustrates the time-averaged ten-day period bias and RMS scores for wind and temperature analyses and forecasts at the 850, 700 and 500 hPa levels in comparison with the observations.

The magnitudes of the bias of the wind and temperature forecasts are relatively small for all vertical levels and forecasts lengths. Furthermore, the bias is rather similar for both of the radar wind runs and the control run. In terms of RMS, however, wind and temperature forecasts using analyses with radar wind observations perform slightly better than the ones without radar wind data, especially at the +24 and +30 h ranges. The improvement occurs both with VAD wind observations and with radar wind super-observations.

There is a large day-to-day variability of the bias and RMS scores with the configurations described above. As an example, Fig. 11 shows the RMS values of the +24 h wind and temperature forecasts at the 850 hPa level, in comparison to the verifying observations for the ten-day period. It is evident that for almost all +24 h forecasts during the period the scores of the runs using radar wind information in either form are superior to the ones not using radar wind data.

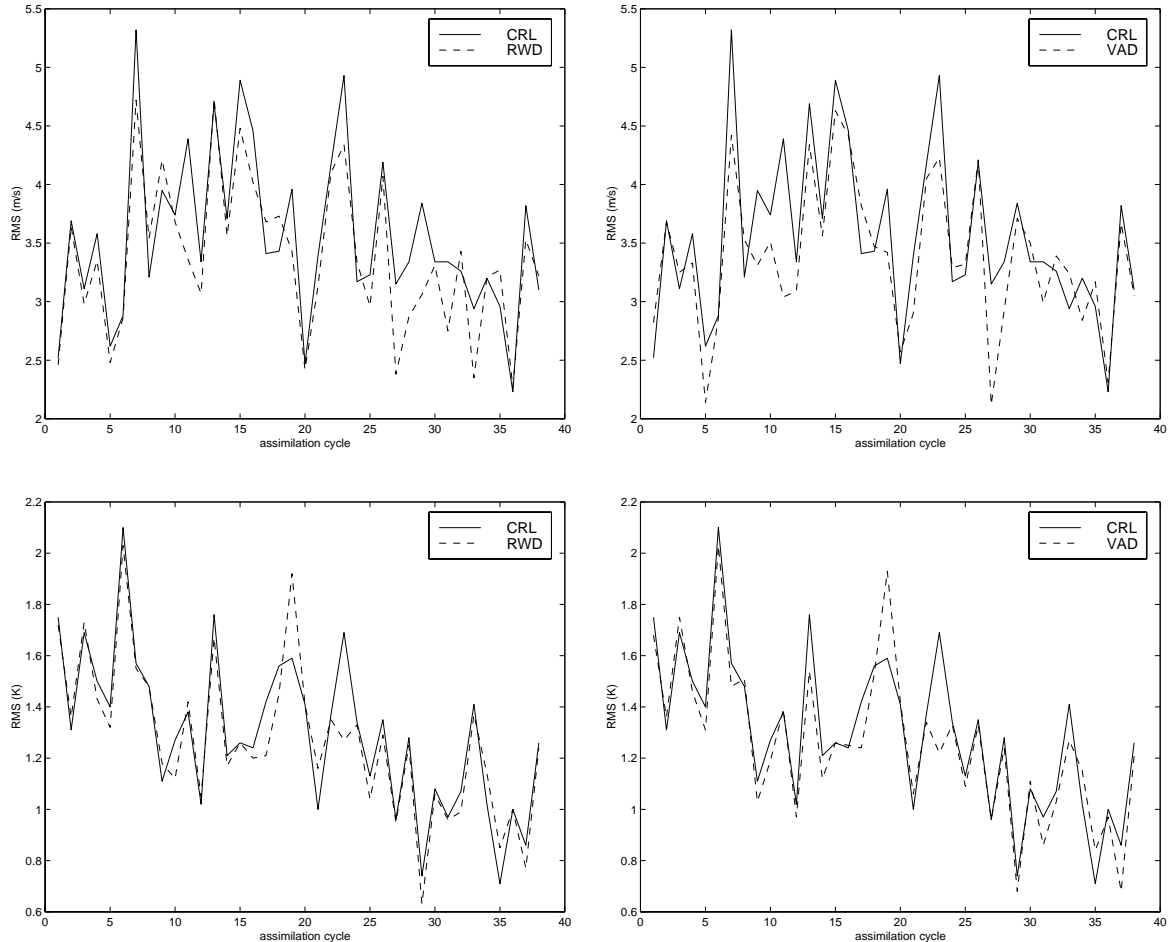


Figure 11: Day-to-day variability of the +24 h 850 hPa wind speed (upper row) and temperature (lower row) RMS scores for the run utilizing conventional observations only (CRL), for the run utilizing conventional observations and radar radial wind super-observations (RWD), and for the run utilizing conventional observations and radar VAD winds (VAD). The units are m/s and K, respectively.

6 Discussion and conclusions

The HIRLAM 3D-Var system has been prepared for assimilation of radar wind data either in the form of radar radial wind super-observations or VAD wind profiles. The observation handling system for radar wind data is designed to be flexible with respect to new requirements for processing and quality control of radar wind data. A randomization method has been applied to obtain a first estimate and a tuning of the radar wind error statistics. Observation fit statistics from a ten-day parallel run reveal a high quality of the radar wind data and reasonably tuned error statistics.

Verification scores from a ten-day parallel run at 22 km horizontal resolution indicate improved forecasts of winds and temperature in the low and middle troposphere, when the forecasts are based on analyses utilizing also radar wind data. The improvement of verification scores is similar when using radar wind observations either as VAD wind profiles or as radial wind super-observations. The impact of radar wind data on surface pressure is rather neutral. It should be kept in mind, however, that in unstable weather situations, like the one illustrated in Fig 8, the incorporation of a number of new observations may affect the large scale analysis in a rather unexpected way. Therefore more extended parallel runs are needed to confirm the promising results obtained here.

It is not possible to use radar wind information in the assimilation both as VAD profiles and as radial wind super-observations because these are based on the same raw data. These two data sources would be redundant through the observation error correlations. It would be impossible to properly account for these error correlations and ignoring them would theoretically degrade the quality of the assimilation and subsequent forecasts.

Future work will include more extended parallel data assimilation experiments, further tuning of error statistics and of the quality control, and preparation of the software for handling of radar wind velocity ambiguities. The latter is needed because of the low unambiguous velocity intervals of many European Doppler radars. De-aliasing may be applied in the processing step, before the generation of super-observations, or it may be handled in the minimization, by the introduction of a multi-modal cost function, for example. The multi-modal cost function would imply of using raw data instead of the super-observations. In addition, the observation operator for radial wind super-observations should be modified to account for the vertical broadening of the radar beam with increasing range from the radar.

7 Acknowledgements

We would like to acknowledge Nils Gustafsson for providing the randomization software for estimation of background errors in observation space and for valuable comments and advice. We also thank Per Undén and the anonymous reviewer for careful reading of the manuscript and for constructive comments.

8 References

- Andersson, E and Järvinen, H, 1999: Variational Quality Control. *Q. J. R. Meteorol. Soc.*, **125**, 697–722.
- Andersson, T, 1992: A method for estimating the wind profile and vertical speed of targets from a single doppler radar. Instruments and observing methods. Report No. 49. *Papers presented at the WMO Technical Conference on Instruments and Methods for Observation (TECO-92). Vienna, Austria, 11-15 May, 1992. WMO/TD-No. 462*, 380–384.
- Browning K A and Wexler, R, 1968: The determination of kinematic properties of a wind field using doppler radar. *J. Appl. Meteorol.*, **7**, 105–113.
- Doviak J D and Dusan, S Z, 1993: Doppler Radar and Weather Observations. Second Edition. *San Diego Academic Press, Inc.*, 562 pp.
- Gilbert, J C and Lemaréchal, C, 1989: Some numerical experiments with variable storage quasi-Newton algorithms. *Math. Prog.*, **B25**, 407–435.
- Gustafsson N, Hörnquist, S, Lindskog, M, Berre, L, Navascués, B, Thorsteinsson, S, Huang, X-Y, Mogensen, K S, Rantakokko, J, 1999: Three dimensional variational data assimilation for a high resolution limited area Model (HIRLAM), HIRLAM Technical report, 40, January 1999, 74 pp.
- Gustafsson, N, Berre, L, Hörnquist, S, Huang, X-Y, Lindskog, M, Navascués, B, Mogensen, K S and Thorsteinsson, S, 2001: Three-dimensional variational data assimilation for a limited area model. Part I: General formulation and the background error constraint. *Tellus*, **53A**, 425–446.
- Henja, A and Michelson, D B, 1999: Improved polar to cartesian radar data transformation. *Preprints AMS 29th Int. Conf. on Radar. Met.*, 252–255.
- Ingleby N B and Lorenc, A C, 1993: Bayesian quality control using multivariate normal distributions. *Q. J. R. Meteorol. Soc.*, **119**, 1195–1225.
- Lhermitte, R M and Atlas, D, 1961: Precipitation motion by pulse Doppler radar. *Proc. 9th Weather Radar Conf., 1961*, **51**, 218–223.
- Lin, C-L, Chai T and Sun, J, 2000: Adjoint Retrieval of Wind and Temperature Fields from a Simulated Convective Boundary Layer. *14th Symposium on Boundary Layer and Turbulence*, Aspen, CO, USA, 7-11 August, 2000, Amer. Meteor. Soc., 106–107.
- Lindskog, M, Järvinen, H and Michelson, D B, 2000: Assimilation of Radar Radial Winds in the HIRLAM 3D-Var. *Phys. Chem. Earth (B)*, **25**, No. 10-12, 1243–1249.
- Lindskog, M, Gustafsson, N, Navascués, B, Mogensen, K S, Huang, X-Y, Yang, X, Andrae, U, Berre, L, Thorsteinsson, S and Rantakokko, J, 2001: Three-dimensional variational data assimilation for a limited area model. Part II: Observation handling and assimilation experiments. *Tellus*, **53A**, 447–468.

- Lorenc, A and Hammon, O, 1988: Objective quality control of observations using Bayesian methods. Theory and practical implementation. *Q. J. R. Meteorol. Soc.*, **114**, 515–543.
- Louis, J F, 1979: A parametric model of vertical eddy fluxes in the atmosphere. *Bound.-Layer meteorol.*, **17**, 187–202.
- Machenhauer, B, 1977: On the dynamics of gravity oscillations in a shallow water model, with application to normal mode initialization. *Beitr. Phys. Atmos.*, **50**, 253–271.
- Michelson, D B, 1999: RAVE User's Guide. Available from SMHI, SE-601 76, Norrköping, Sweden. 51 pp..
- Michelson, D B, Andersson, T, Koistinen, J, Collier, C G, Riedl, J, Szuruc, J, Gjertsen, U, Nielsen, A and Overgaard, S, 2000: BALTEX Radar Data Centre Products and their Methodologies. *RMK 90 SMHI, SE-601 76 Norrköping*, 76 pp.
- Parrish, D F and Derber, J C, 1992: The National Meteorological Centre's spectral statistical interpolation analysis system. *Mon. Wea. Rev.*, **120**, 1747–1763.
- Parrish, D F and Purser, J, 1998: Anisotropic Covariances in 3D-VAR: Application to Hurricane Doppler Radar Observations. *Workshop report from HIRLAM 4 Workshop on Variational Analysis in Limited Area Models, Meteo-France, Toulouse 23-25 February, 1998*.
- Rossa, A, 2000: COST-717: Use of Radar Observations in Hydrological and NWP Models. *Phys. Chem. Earth (B)*, **25**, No. 10-12, 1221-1224.
- Saarinen, S, Vasiljević, D and Järvinen, H, 1997: Parallelization of observation processing. In: Making its mark. Proceedings of the Seventh ECMWF Workshop on the Use of Parallel Processors in Meteorology. Eds. G-R Hoffman and N Kreitz. World Scientific Publishing Co, London. pp. 52–67.
- Savijärvi, H, 1989: Fast Radiation Parameterization Schemes for Mesoscale and Short-Range Forecast Models. *J. Appl. Meteor.*, **29**, 437–447.
- Sun, J and Crook, N A, 1997: Dynamical and microphysical retrieval from Doppler radar observations using a cloud model and its adjoint: Part I. model development and simulated data experiments. *J. Atmos. Sci.*, **54**, 1642–1661.
- Sundqvist H, Berge, E and Kristjansson, J E, 1989: Condensation and cloud parameterization studies with a mesoscale numerical weather prediction model. *Mon. Wea. Rev.*, **117**, 1641–1657.